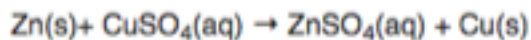


Oxidation/Reduction Metal Displacement Reaction

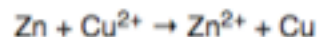
Metal displacement [\[edit \]](#)

In this type of reaction, a metal atom in a compound (or in a solution) is replaced by an atom of another metal. For example, **copper** is deposited when **zinc** metal is placed in a **copper(II) sulfate** solution:

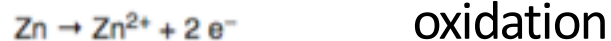


In the above reaction, zinc metal displaces the copper(II) ion from copper sulfate solution and thus liberates free copper metal.

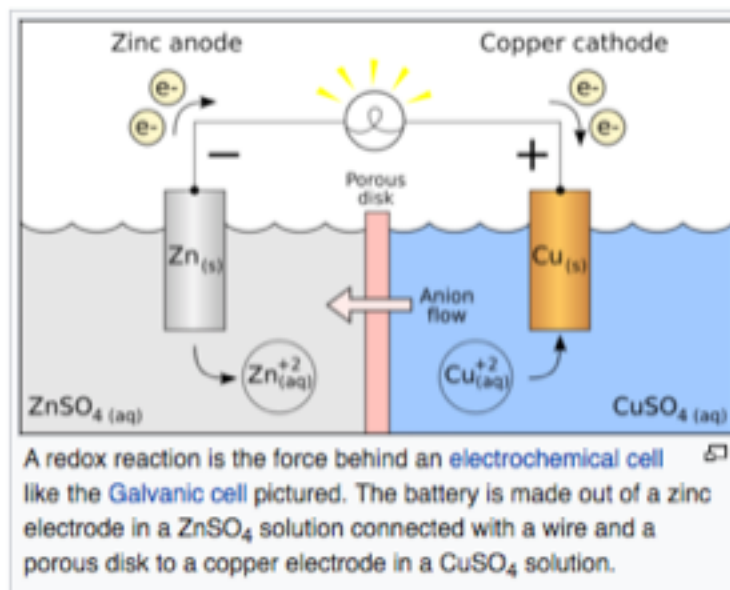
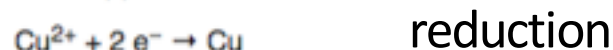
The ionic equation for this reaction is:



As two **half-reactions**, it is seen that the zinc is oxidized:



And the copper is reduced:



1.10 Volts for each cell

Activity Series of Metals (in Order of Reactivity)

Element **Oxidation Half Reaction**

Lithium $\text{Li}(s) \rightarrow \text{Li}^+(aq) + e^-$

Most active or most easily oxidized

Potassium $\text{K}(s) \rightarrow \text{K}^+(aq) + e^-$

Barium $\text{Ba}(s) \rightarrow \text{Ba}^{2+}(aq) + 2e^-$

Calcium $\text{Ca}(s) \rightarrow \text{Ca}^{2+}(aq) + 2e^-$

Sodium $\text{Na}(s) \rightarrow \text{Na}^+(aq) + e^-$

Magnesium $\text{Mg}(s) \rightarrow \text{Mg}^{2+}(aq) + 2e^-$

Aluminum $\text{Al}(s) \rightarrow \text{Al}^{3+}(aq) + 3e^-$

Zinc $\text{Zn}(s) \rightarrow \text{Zn}^{2+}(aq) + 2e^-$

-0.76 V
←

Iron $\text{Fe}(s) \rightarrow \text{Fe}^{2+}(aq) + 2e^-$

Nickel $\text{Ni}(s) \rightarrow \text{Ni}^{2+}(aq) + 2e^-$

Tin $\text{Sn}(s) \rightarrow \text{Sn}^{2+}(aq) + 2e^-$

Lead $\text{Pb}(s) \rightarrow \text{Pb}^{2+}(aq) + 2e^-$

Hydrogen $\text{H}_2(g) \rightarrow 2\text{H}^+(aq) + 2e^-$

Copper $\text{Cu}(s) \rightarrow \text{Cu}^{2+}(aq) + 2e^-$

0.34 V
←

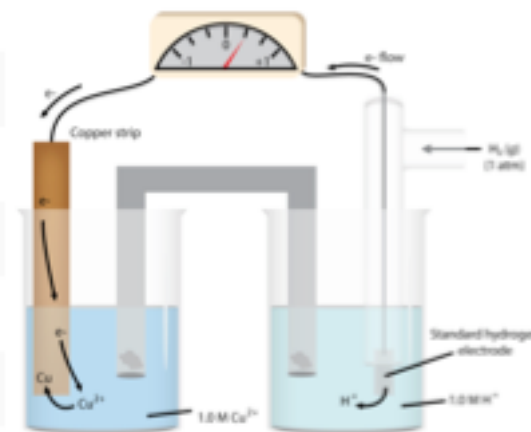
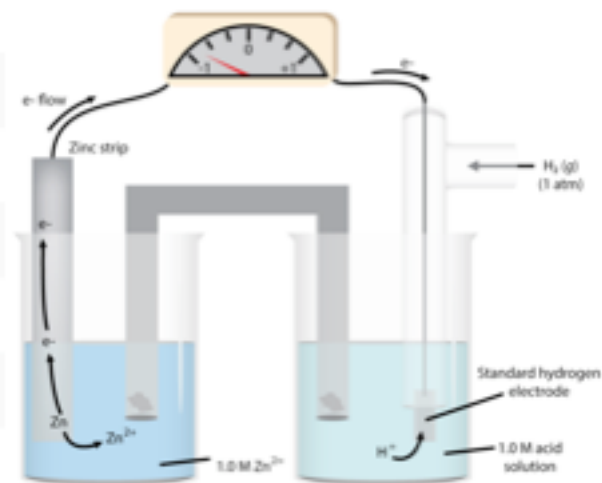
Mercury $\text{Hg}(l) \rightarrow \text{Hg}^{2+}(aq) + 2e^-$

Silver $\text{Ag}(s) \rightarrow \text{Ag}^+(aq) + e^-$

Platinum $\text{Pt}(s) \rightarrow \text{Pt}^{2+}(aq) + 2e^-$

Gold $\text{Au}(s) \rightarrow \text{Au}^{3+}(aq) + 3e^-$

Least active or most difficult to oxidize

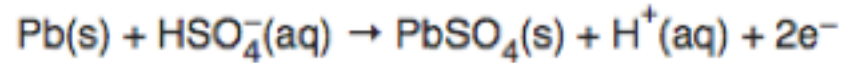


$$E^{\circ}_{\text{cell}} = 0.34 \text{ V (copper)} - (-0.76 \text{ V zinc}) = 1.10 \text{ volts for the cell}$$

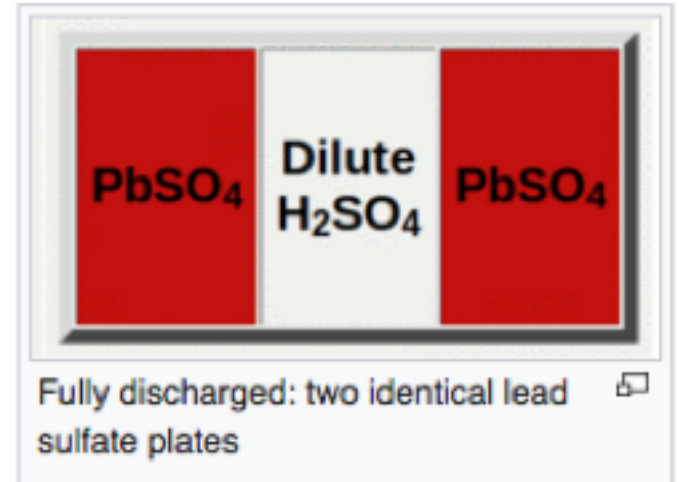
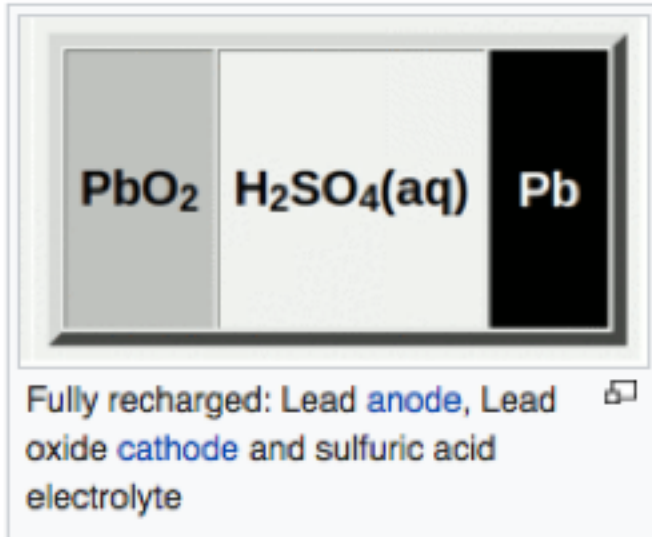
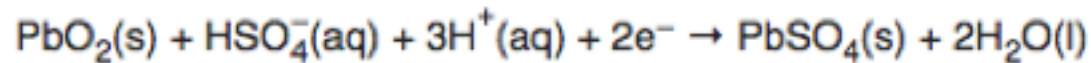
Standard Reduction Potentials at 25°C	
Half Reaction	E° (V)
$F_2 + 2e^- \rightarrow 2F^-$	+2.87
$PbO_2 + 4H^+ + SO_4^{2-} + 2e^- \rightarrow PbSO_4 + 2H_2O$	+1.70
$MnO_4^- + 8H^+ + 5e^- \rightarrow Mn^{2+} + 4H_2O$	+1.51
$Au^{3+} + 3e^- \rightarrow Au$	+1.50
$Cl_2 + 2e^- \rightarrow 2Cl^-$	+1.36
$Cr_2O_7^{2-} + 14H^+ + 6e^- \rightarrow 2Cr^{3+} + 7H_2O$	+1.33
$O_2 + 4H^+ + 4e^- \rightarrow 2H_2O$	+1.23
$Br_2 + 2e^- \rightarrow 2Br^-$	+1.07
$NO_3^- + 4H^+ + 3e^- \rightarrow NO + 2H_2O$	+0.96
$2Hg^{2+} + 2e^- \rightarrow Hg_2^{2+}$	+0.92
$Hg^{2+} + 2e^- \rightarrow Hg$	+0.85
$Ag^+ + e^- \rightarrow Ag$	+0.80
$Fe^{3+} + e^- \rightarrow Fe^{2+}$	+0.77
$I_2 + 2e^- \rightarrow 2I^-$	+0.53
$Cu^+ + e^- \rightarrow Cu$	+0.52
$O_2 + 2H_2O + 4e^- \rightarrow 4OH^-$	+0.40
$Cu^{2+} + 2e^- \rightarrow Cu$	+0.34
$Sn^{4+} + 2e^- \rightarrow Sn^{2+}$	+0.13
$2H^+ + 2e^- \rightarrow H_2$	0.00
$Pb^{2+} + 2e^- \rightarrow Pb$	-0.13
$Sn^{2+} + 2e^- \rightarrow Sn$	-0.14
$Ni^{2+} + 2e^- \rightarrow Ni$	-0.25
$Co^{2+} + 2e^- \rightarrow Co$	-0.28
$PbSO_4 + 2e^- \rightarrow Pb + SO_4^{2-}$	-0.31
$Cd^{2+} + 2e^- \rightarrow Cd$	-0.40
$Fe^{2+} + 2e^- \rightarrow Fe$	-0.44
$Cr^{3+} + 3e^- \rightarrow Cr$	-0.74
$Zn^{2+} + 2e^- \rightarrow Zn$	-0.76
$2H_2O + 2e^- \rightarrow H_2 + 2OH^-$	-0.83
$Mn^{2+} + 2e^- \rightarrow Mn$	-1.18
$Al^{3+} + 3e^- \rightarrow Al$	-1.66
$Be^{2+} + 2e^- \rightarrow Be$	-1.70
$Mg^{2+} + 2e^- \rightarrow Mg$	-2.37
$Na^+ + e^- \rightarrow Na$	-2.71
$Ca^{2+} + 2e^- \rightarrow Ca$	-2.87
$Sr^{2+} + 2e^- \rightarrow Sr$	-2.89
$Ba^{2+} + 2e^- \rightarrow Ba$	-2.90
$Rb^+ + e^- \rightarrow Rb$	-2.92
$K^+ + e^- \rightarrow K$	-2.92
$Cs^+ + e^- \rightarrow Cs$	-2.92
$Li^+ + e^- \rightarrow Li$	-3.05

Deep Cycle Lead Acid Battery Manufacture

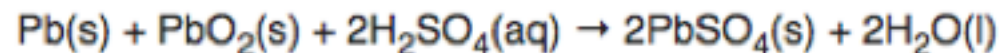
Negative plate reaction



Positive plate reaction

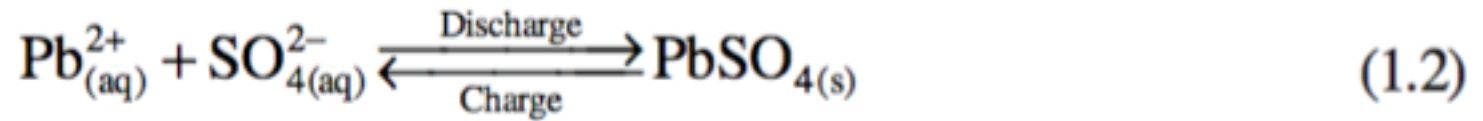
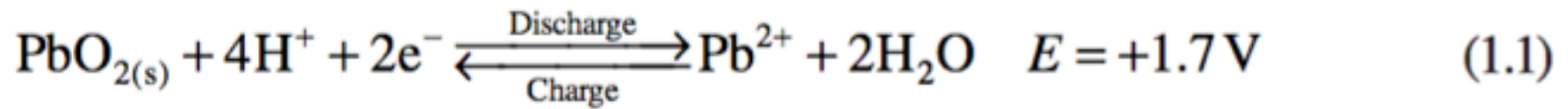


The total reaction can be written as



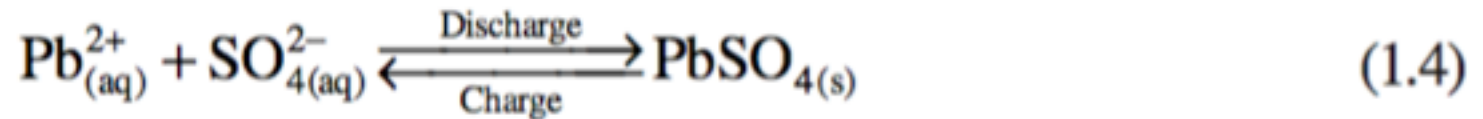
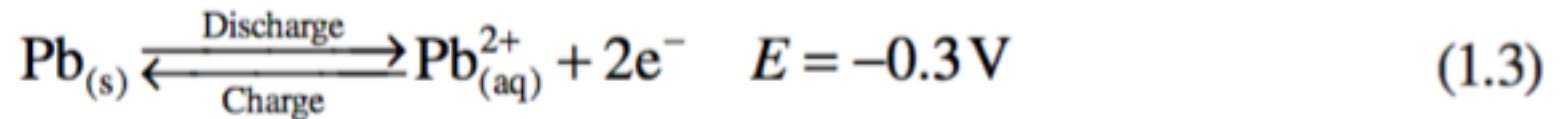
[Lead Acid Battery Technologies \(eBook at UC\)](#)

Reduction

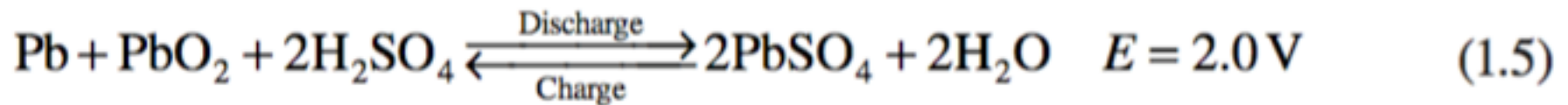


Negative electrode (cathode):

Oxidation



Overall reaction:



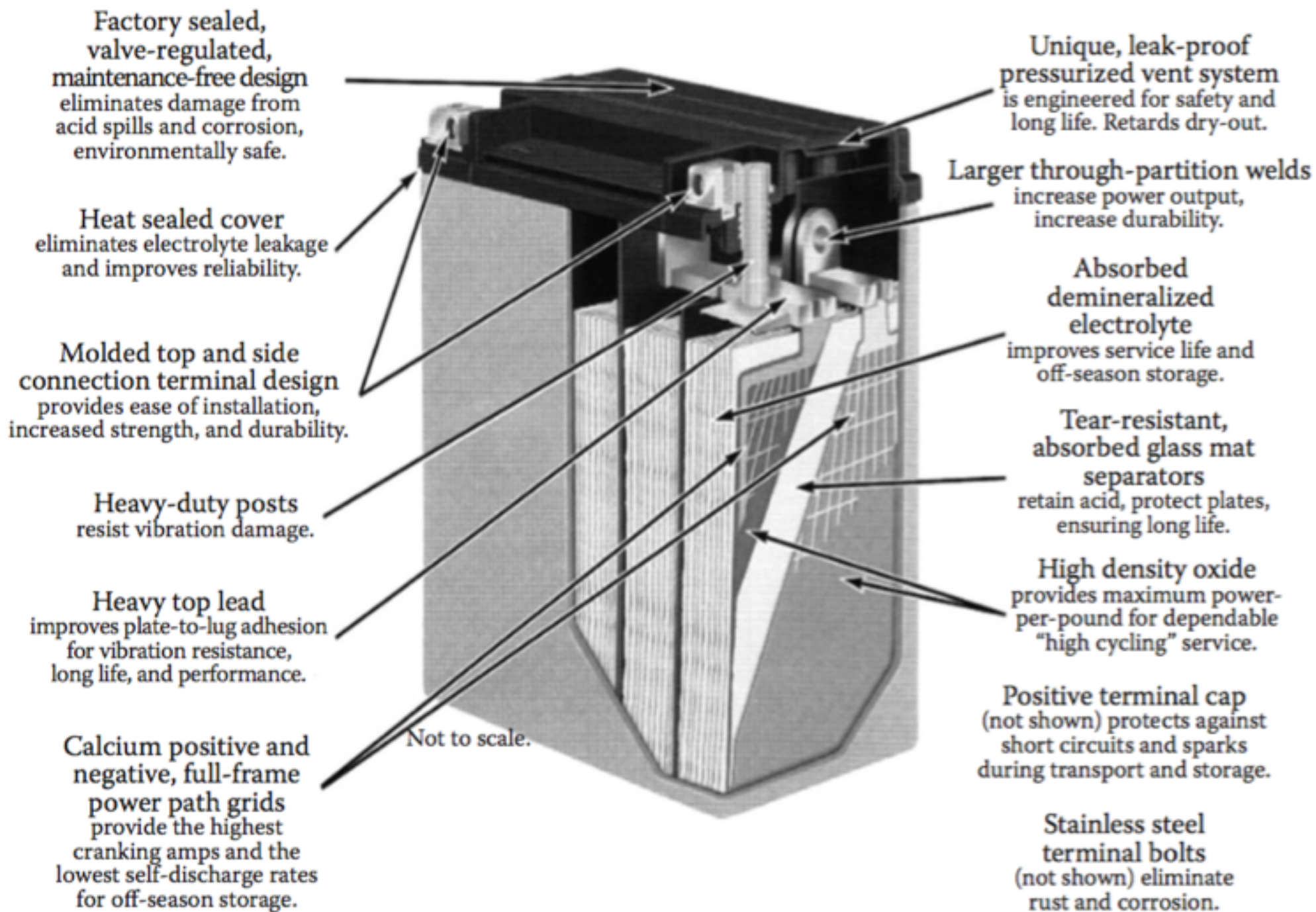


FIGURE 1.1 Cut-away of lead-acid battery. (From East Penn Manufacturing Co.)

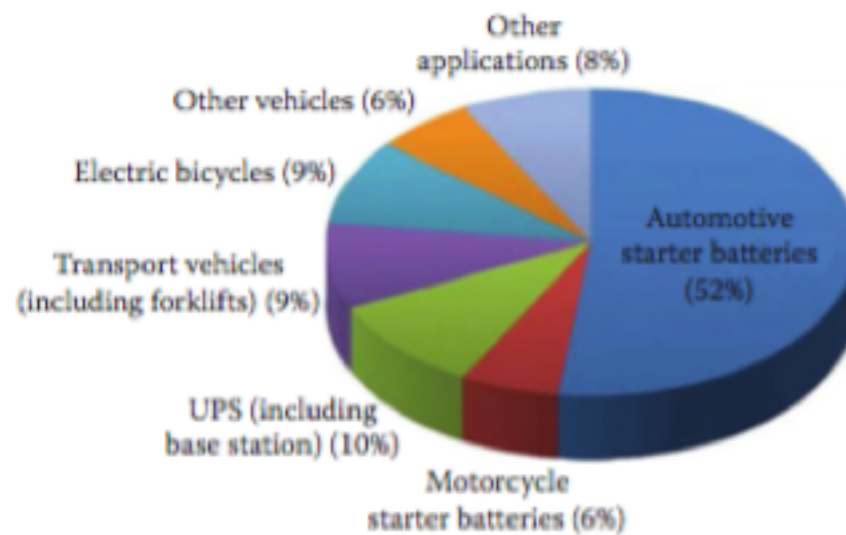


FIGURE 10.1 Lead-acid battery market application category ratio. (Available at <http://www.systems-sunlight.com/blog/global-lead-acid-battery-market-development-status>.)

10.2 LEAD BATTERIES IN APPLICATIONS

10.2.1 TYPES OF LEAD-ACID BATTERIES

The many different types of lead-acid batteries on the market are used for various applications. The major types of lead-acid batteries can be described as follows [3]:

1. *Valve-regulated lead-acid (VRLA) batteries.* Also called *sealed lead-acid (SLA) batteries*, the VRLA batteries can prevent electrolyte evaporation loss, spillage, and gassing, which leads to a prolonged maintenance-free life span. The top of the battery has a capped vent that is used for the escape of gas. It also has some pressure valves that can open only under extreme conditions. This type of battery uses a specially designed electrolyte to reduce the release of gases such as oxygen and hydrogen generated by the side reactions that occur during charging. A recombinant system with a catalyst inside the battery is needed to facilitate the combination reaction between hydrogen and oxygen to recombine into water. This type of battery is normally safer than other types because the acid electrolyte spoilage is eliminated. This type of battery is used mainly in automobiles.
2. *Absorbed glass mat (AGM) batteries.* Also known as *absorptive glass microfiber (AGMF) batteries*, this type of battery belongs to the class of VRLA batteries, but it has a boron silicate fiber glass mat that acts as a separator between the electrodes, which can absorb the free electrolyte in much the same way a sponge absorbs water. This separator can promote recombination of the hydrogen and oxygen produced during the charging process. The fiber glass mat can absorb and immobilize the acid in the mat as a form of liquid rather than a gel form, therefore, there is no gel electrolyte in this type of battery. Furthermore, in the presence of such a mat separator, the acid electrolyte is more readily available to the plates, allowing for faster reactions between the acid and the plate material, resulting in higher charge–discharge rates as well as deep cycling. In addition, because the electrolyte is kept inside the mat separator, the battery is more robust and able to withstand severe shock and vibration without leakage even if the case is cracked. To realize this, the fiber glass mat separator is normally 95% saturated with sulfuric acid with excess electrolyte. For this reason, AGM batteries are also sometimes called “starved electrolyte” or “dry” batteries.
3. *Gel batteries.* This type of battery also belongs to the class of VRLA batteries. The acid electrolyte is in the form of a gel, however, rather than mobile liquid, which promotes oxygen recombination. In addition, batteries that use a gel as the electrolyte are more robust.

4. *Starting, lighting, and ignition (SLI) batteries.* SLI batteries are specially designed for automobile starting-lighting-ignition applications. The design does not allow the battery to be discharged below 50% depth of discharge (DOD) because discharging below these levels could damage the plates and shorten battery life. In general, automotive batteries are always fully charged before starting the car. After starting the vehicle, the lost charge, typically 2% to 5% of the charge, is immediately replaced by the alternator and the battery returns to the fully charged state.
5. *Deep-cycle batteries.* Deep-cycle batteries are designed to be completely discharged before recharging. This is required by applications such as marine applications, golf carts, forklifts, and electric vehicles, where the batteries could be deeply cycled. In this deep-cycling process, excessive heat is produced, which can warp the plates. Therefore, thicker and stronger or solid plate grids are normally used for deep-cycle applications.

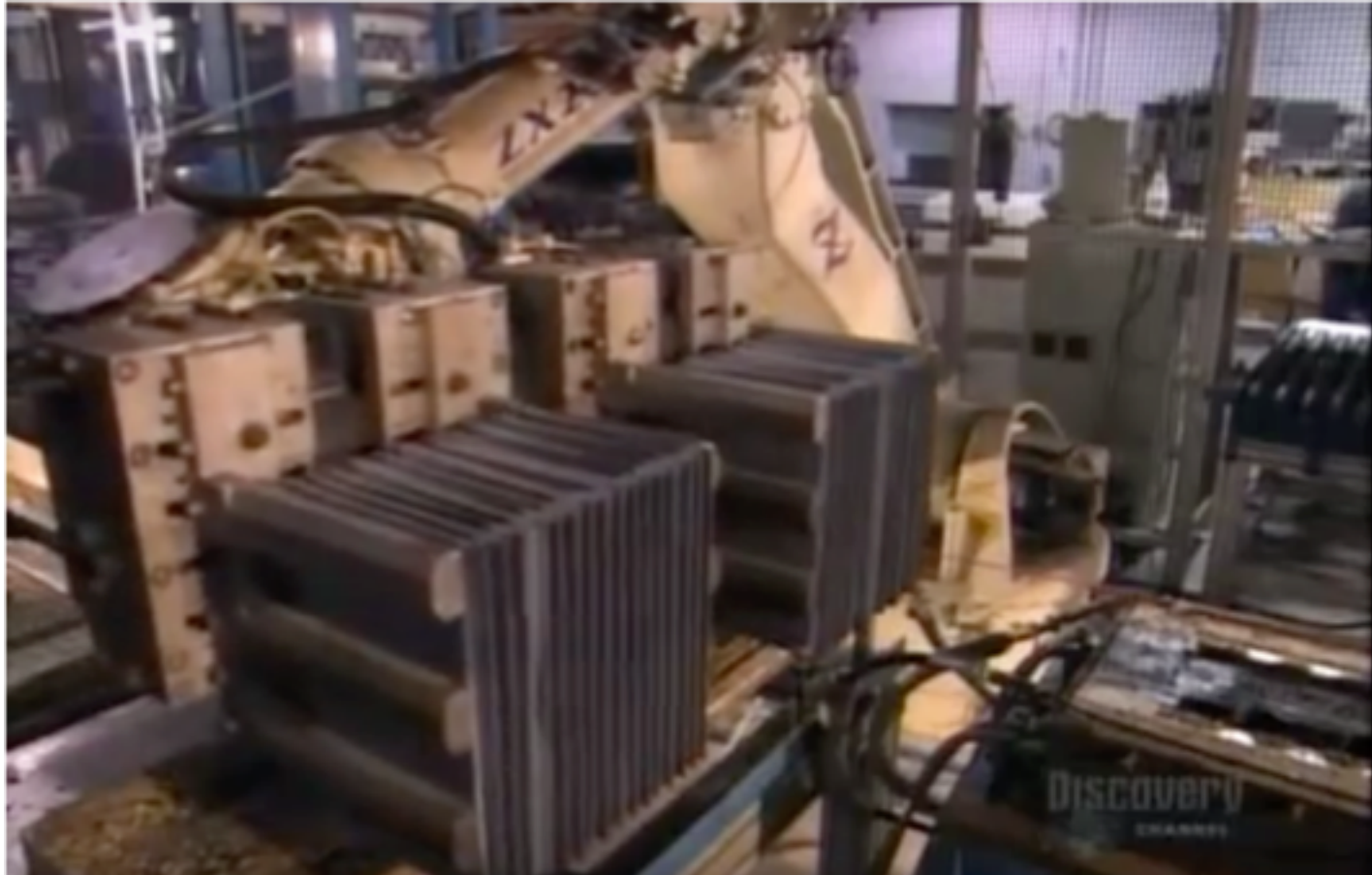
Gelled electrolytes [\[edit \]](#)

Main article: [VRLA battery § Gel_battery](#)

During the 1970s, researchers developed the sealed version or "gel battery", which mixes a silica gelling agent into the electrolyte (silica-gel based lead-acid batteries used in portable radios from early 1930s were not fully sealed). This converts the formerly liquid interior of the cells into a semi-stiff paste, providing many of the same advantages of the AGM. Such designs are even less susceptible to evaporation and are often used in situations where little or no periodic maintenance is possible. Gel cells also have lower freezing and higher boiling points than the liquid electrolytes used in conventional wet cells and AGMs, which makes them suitable for use in extreme conditions.

The only downside to the gel design is that the gel prevents rapid motion of the ions in the electrolyte, which reduces carrier mobility and thus surge current capability. For this reason, gel cells are most commonly found in energy storage applications like off-grid systems.

Deep Cycle Battery Manufacture in the Developed World



[Battery Manufacture in Nepal Part 1](#)

[Battery Manufacture in Nepal Part 2](#)



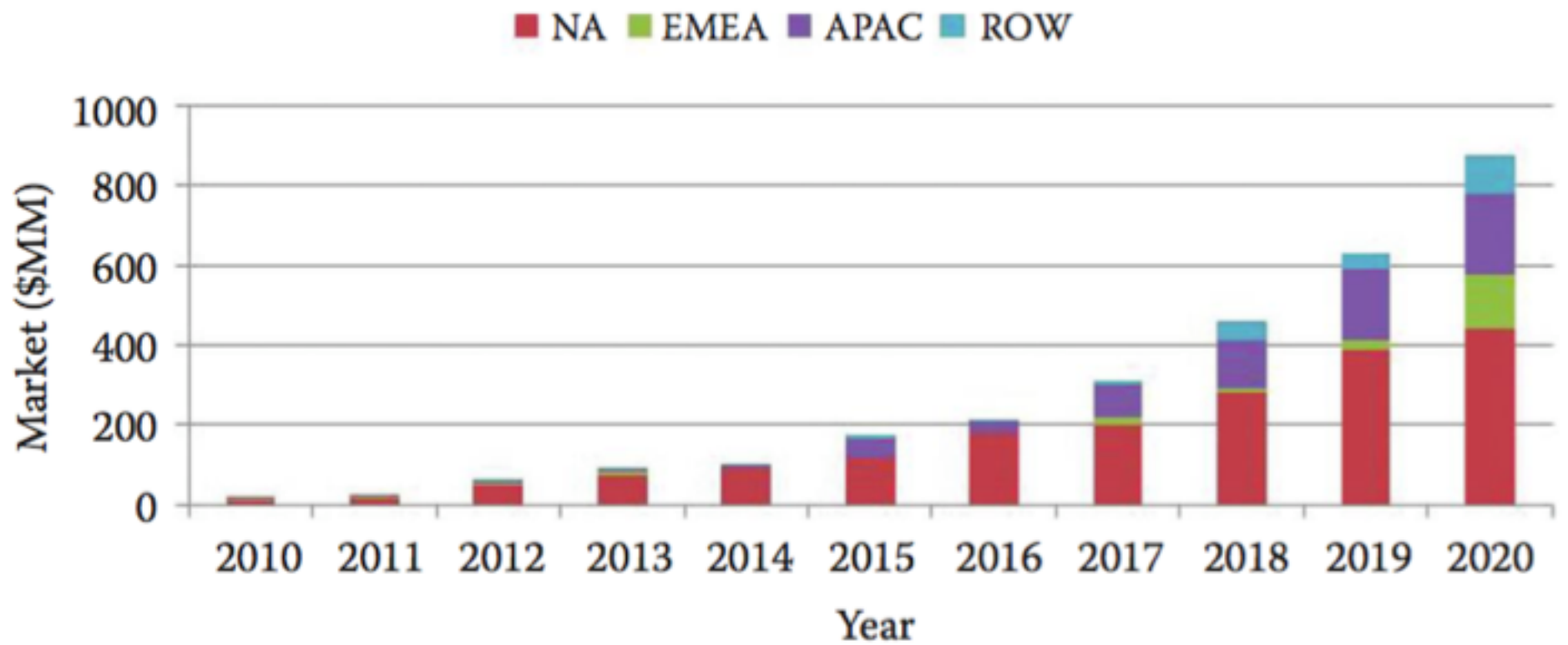


FIGURE 1.7 Emerging grid battery market projection.

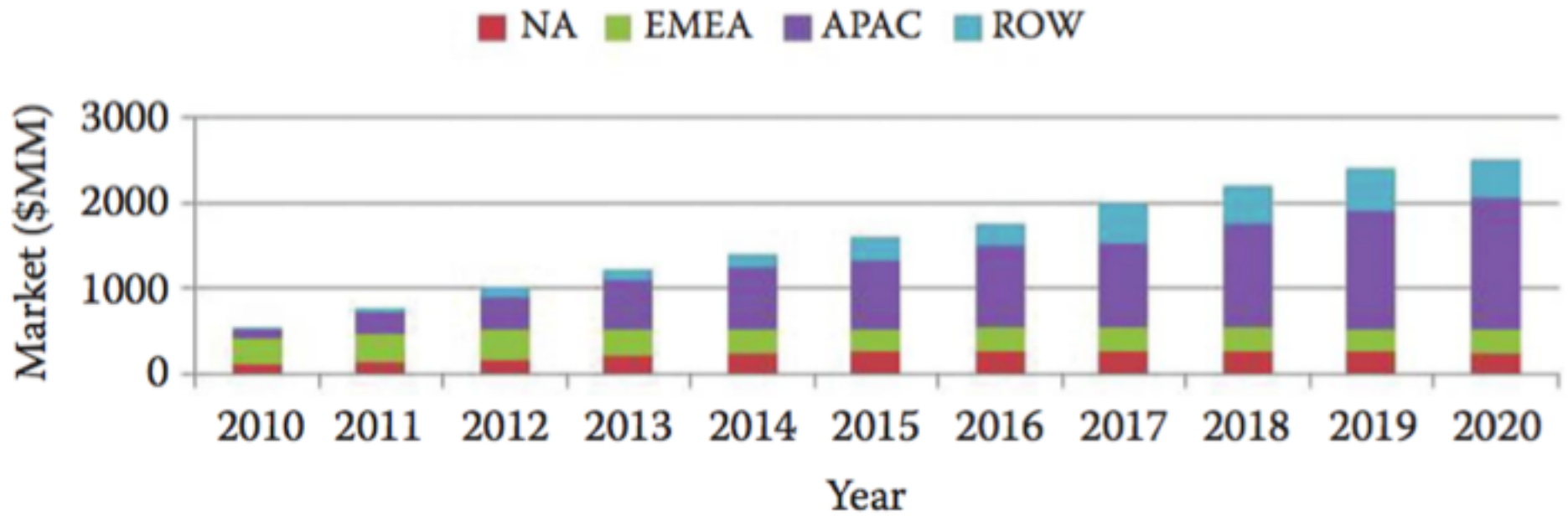


FIGURE 1.8 Distributed renewable battery market projection.

Battery manufacturing process flowchart
 concast/wet (jar) formation
 (Not used for dry charge!)

Vitriol = Sulfate

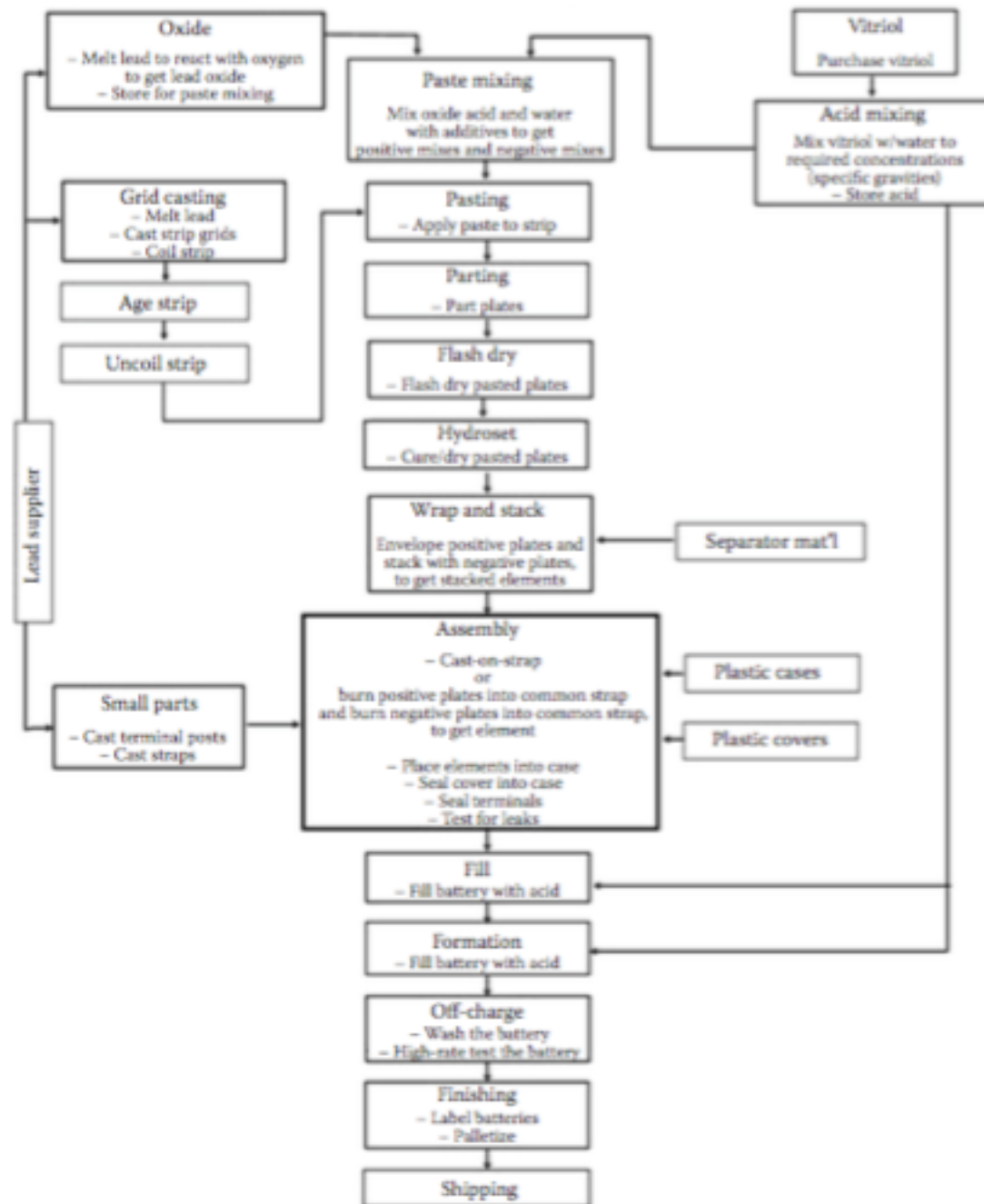


FIGURE 1.23 Battery assembly process. (From <http://www.docstoc.com>.)



FIGURE 7.1 Battery manufacturing process. (From International Thermal Systems. Available at <http://internationalthermalsystems.com/batterymanufacturing>.)

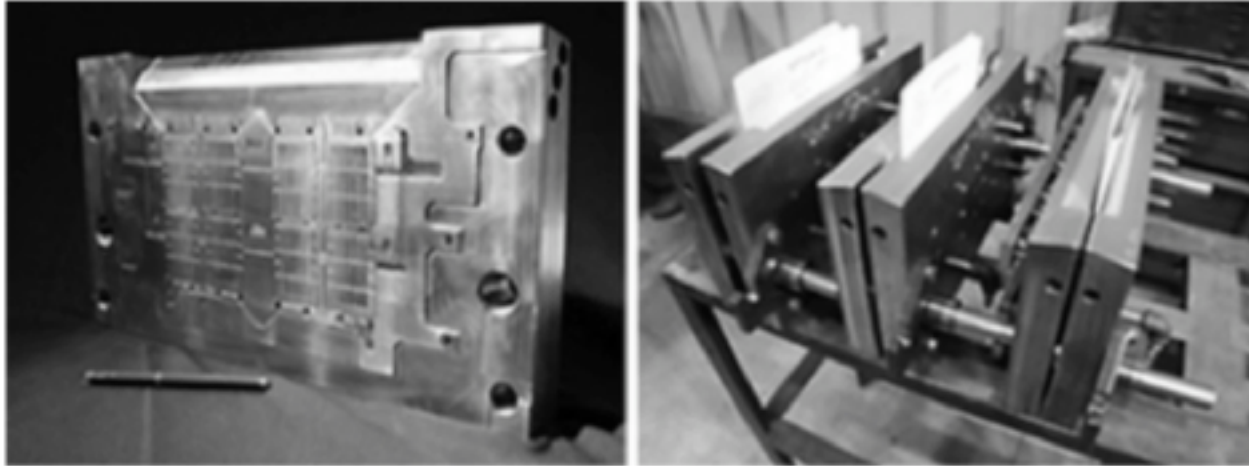


FIGURE 7.2 Battery grid casting mold (book mold). (From Wirtz Manufacturing. Available at <http://www.wirtzusa.com>.)



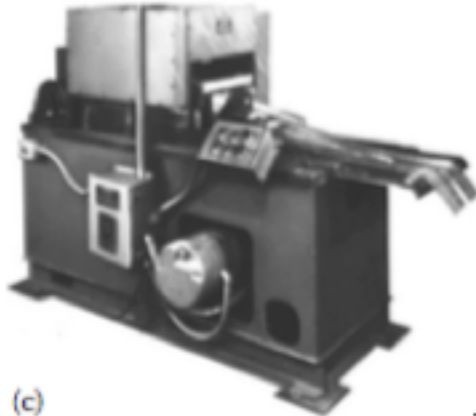
FIGURE 7.3 Book mold grid caster. (From Wirtz Manufacturing. Available at <http://www.wirtzusa.com>.)



(a)



(b)



(c)



(d)

FIGURE 7.4 Strip expansion process equipment. (a) Lead-alloy strip caster: Multialloy caster produces fully edge-trimmed lead alloy strips; (b) Coil feeder: This machine feeds the coiled lead from the horizontal position; (c) Expander: Using a die, the expander produces controlled expansion, which results in the grid's diamond pattern and height; (d) Shaper: The shaper forms the lugs and accurately sizes the grid for height and thickness. A positive feed mechanism aligns and positions the expanded strip and a punch-and-die knocks out clean, reclaimable lead from the unexpanded center portion of the strip. (From MAC Engineering. Available at <http://www.mac-eng.com>; Battery Technology Solutions Inc. Available at <http://www.batechsol.com>.)



FIGURE 7.6 Continuous grid caster. (From Wirtz Manufacturing. Available at <http://www.wirtzusa.com>.)

7.2 LEAD OXIDE PRODUCTION

Lead oxide is the main component of the active material for both positive and negative electrodes. Lead oxide is made by oxidizing lead using either the Barton pot process or the Ball mill process.

7.2.1 BARTON POT PROCESS

The Barton pot process (also called the Barton-like process) is a process that melts lead ingots and feeds them into a vessel or pot. The molten lead is rapidly stirred and atomized into very small droplets via a rotating paddle in proximity to the bottom of the vessel. The droplets of molten lead are then oxidized by oxygen in the air to produce an oxide coating around the droplet. Figure 7.7 shows a flowchart for the Barton pot process.

The lead oxidation process is exothermic and the generated heat is essential for sustaining a continuous reaction as more lead is introduced. The process temperature is critical for determining the degree of oxidation and crystal morphology of the lead oxide. The Barton pot process typically produces a product containing lead oxide with 15% to 30% free lead, which exists as the core of the lead oxide spherically shaped particles. Figure 7.8 shows a Barton pot.

7.2.2 BALL MILL PROCESS

In the Ball mill process, as shown in Figure 7.9, lead pieces are fed into a rotating mill and the attrition of the lead pieces produces fine metallic lead flakes. The friction of lead flakes tumbling against each other inside the mill chamber creates sufficient heat to oxidize the lead flakes' surfaces. The degree of lead oxidation is impacted by the airflow through the system. The airflow also moves the lead oxide particles to be collected in a baghouse. The product of the Ball mill process contains 15% to 30% free lead in the shape of a flattened platelet core surrounded by an oxide coating. Figure 7.10 shows a Ball mill [3,5].

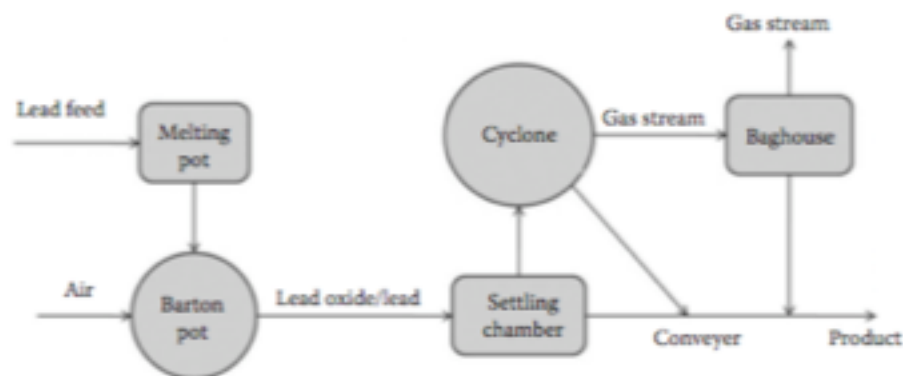


FIGURE 7.7 Flowchart of the Barton pot process.



FIGURE 7.8 Barton pot. (From Wirtz Manufacturing. Available at <http://www.wirtzusa.com>.)

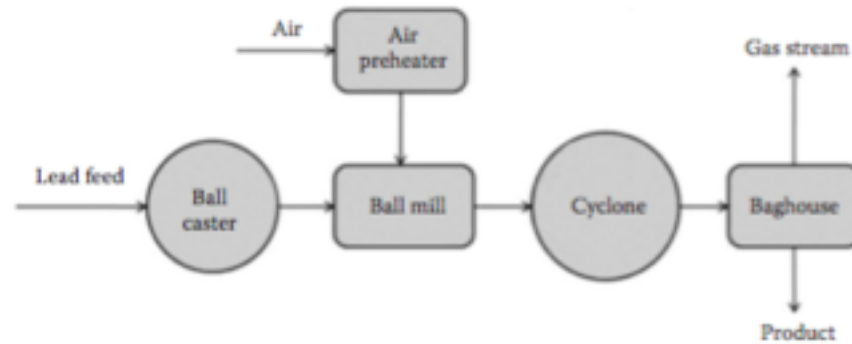


FIGURE 7.9 Flowchart of Ball mill process.



FIGURE 7.10 Ball mill. (From MAC Engineering. Available at <http://www.mac-eng.com>; Leader Tech United. Available at <http://www.ltucompany.com>.)

TABLE 7.1
Lead Oxide Characteristics of the Products of the Barton Pot and Ball Mill Processes

Characteristic	Barton Pot	Ball Mill
Particle size	3–4 mm in diameter	2–3 mm in diameter
Stability/reactivity in air	Stable	High reactivity in air
Oxide crystal structures (wt%)	5–30% β -PbO, remaining balance α -PbO	100% α -PbO
Acid adsorption (mg H ₂ SO ₄ /g oxide)	160–200	240
Surface area (m ² /g)	0.7	2.0–3.0
Free lead content (wt%)	18–28	25–35
Paste mixing characteristics	Softer paste	Stiffer paste
Paste curing	Average curing rate	Faster curing rate
Battery performance	Better battery life, low capacity	Good capacity, shorter life
Deep-cycle ability	Usually good	Sometimes good
Process control	More difficult	Easier
Production rate (kg/h)	300–900	1000
Operating costs	Low operating and maintenance costs	Higher operating and maintenance costs
Facility requirement	Smaller footprint	Bigger footprint
Energy consumption (kWh/ton)	Up to 100	100–300

Table 7.1 lists the lead oxide characteristics produced by the Barton pot and Ball mill processes.

7.3.1 BATCH PASTE MIXER

Conventional mechanical mixers are batch type. The major types of mechanical mixers are the pony mixer, the muller, or the vertical muller (Figure 7.11). The batch paste mixer contains three major components: the paste tank, mixing system, and cooling system.

1. *Paste tank.* The paste tank is a closed cylindrical steel tank. The upper part of the tank has inspection doors and hoses for cooling air inlet and outlet. There are also pipes for the inlet of acid and water. The sides of the tank have two discharging doors that are used to dump the final prepared paste into the cone feeder.
2. *Mixing system.* The mixing system contains rotating paddles, which provide a complete mixing action of the various components (lead, acid, water, and additives/expanders) to obtain a uniform and easily pasted paste.



FIGURE 7.11 Vertical muller mixer. (From MAC Engineering. Available at <http://www.mac-eng.com>.)

3. *Cooling system.* In the mixing cycle, cooling is essential because heat is generated by the exothermic reaction between H_2SO_4 and lead oxide. Failure to maintain proper paste temperature causes hardening of the paste before it can be used. The temperature of the paste needs to be controlled, and this is often achieved by either cooling the mixer or evaporating the extra volume of water in the paste mixture. It is important to maintain the mixing temperature to ensure a good-quality paste results. Often, two types of cooling systems are used in the paste mixing system. The first cooling system, an air-conditioning (AC) system, uses a fan blowing over the paste surface for cooling. The second cooling system uses circulating water that runs through the bottom and surrounding area of the tank to maintain the desired temperature/cooling. The peak temperature limit for the pasting cycle is $60^\circ C$, whereas the final paste or dumping paste temperature should be less than $50^\circ C$.

The paste viscosity will rise in the beginning of paste mixing, but then gradually decreases. The ratio of lead oxide, water, and sulfuric acid varies depending on the type of battery applications. For example, plates for SLI application are generally made at a low $PbO:H_2SO_4$ ratio, whereas plates for deep-cycle applications are made at a high $PbO:H_2SO_4$ ratio. On the other hand, the amount of sulfuric acid affects the plate density because the more acid used, the lower the plate density. Paste density is measured by using a cup with a hemispherical cavity and by the measurement of paste consistency (viscosity) with a penetrometer.

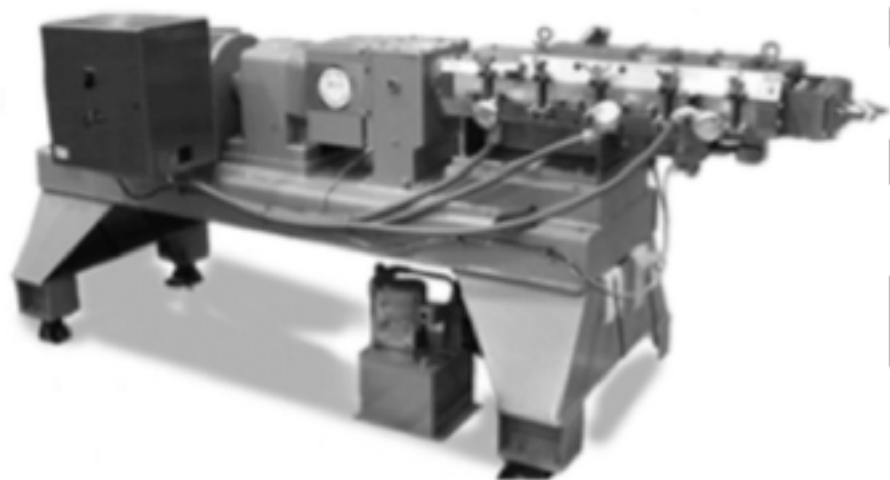


FIGURE 7.12 Continuous paste mixer. (From Battery Technology Solutions Inc. Available at <http://www.batechsol.com>.)



FIGURE 7.13 Continuous belt pasteur. (From Wirtz Manufacturing. Available at <http://www.wirtzusa.com>.)

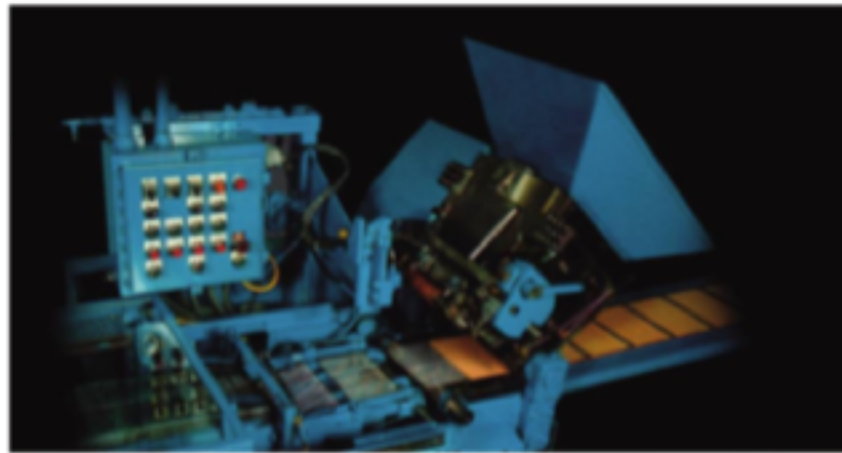
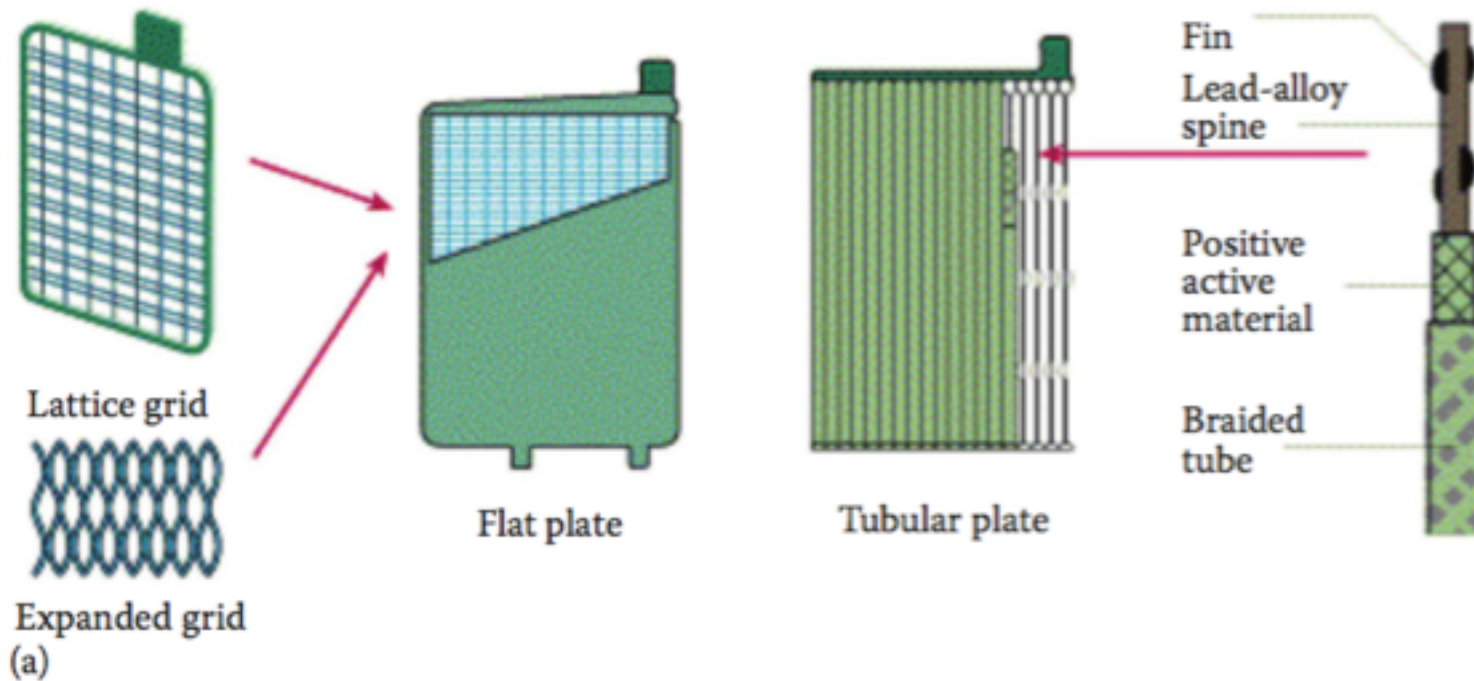


FIGURE 7.14 Continuous orifice paster. (From Wirtz Manufacturing. Available at <http://www.wirtzusa.com>.)

1.7.2 DEEP-CYCLE AND TRACTION BATTERIES

Deep-cycle batteries require good cycle life, high energy density, and low cost. The cycle life of a deep-cycle battery is usually longer than that of an SLI battery. The longer cycle life is achieved in the following manner:

1. Use thick plates with high paste density.
2. Cure the plates with a high-temperature and high-humidity profile.
3. Employ a low-specific-gravity electrolyte for formation.



(b)

FIGURE 3.1 Lead-acid battery electrode structures: (a) flat and tubular plates; (b) pasted flat electrode, in which the two grids on the left are made of carbon and lead, respectively. After the grid is pasted and cured, the electrode is formed as shown at right. ([a] From <http://www.checkthatcar.com/carfaq2.asp>. [b] From A. Kirchev et al., *J. Power Sources*, 196(20), 8773–8788, 2011.)

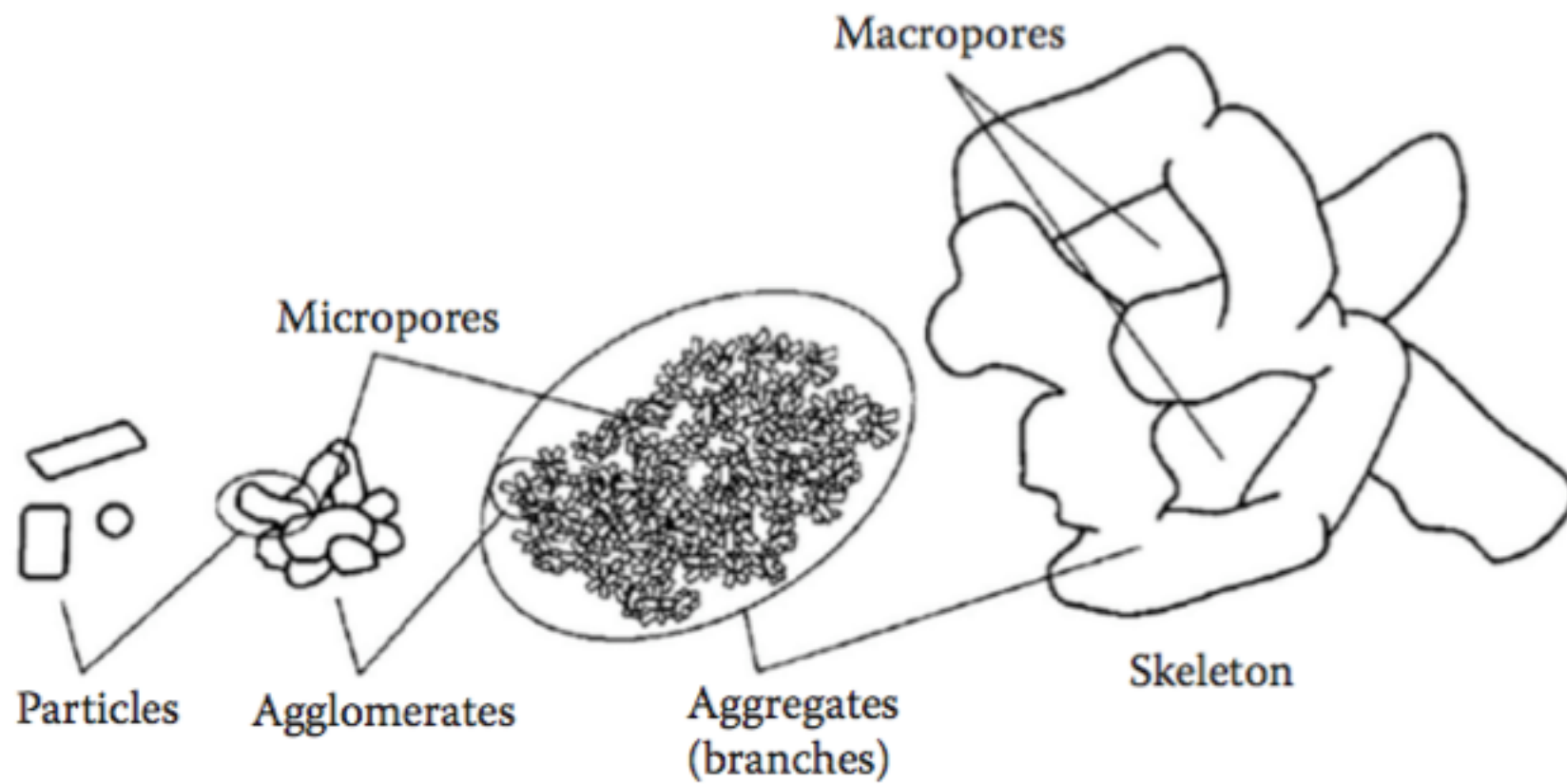


FIGURE 3.3 Structure of the lead dioxide active mass. (From D. Pavlov, and E. Bashtavelova, *J. Electrochem. Soc.*, 131, 1468, 1984; D. Pavlov, and E. Bashtavelova, *J. Electrochem. Soc.*, 133, 241, 1986; D. Pavlov et al., "Structure of the Lead-Acid Battery Active Masses," in *Proc. Int. Symp. Advances in Lead-Acid Batteries*, Vol. 84-14, p. 16, Electrochemical Society, Pennington, NJ, 1984.)

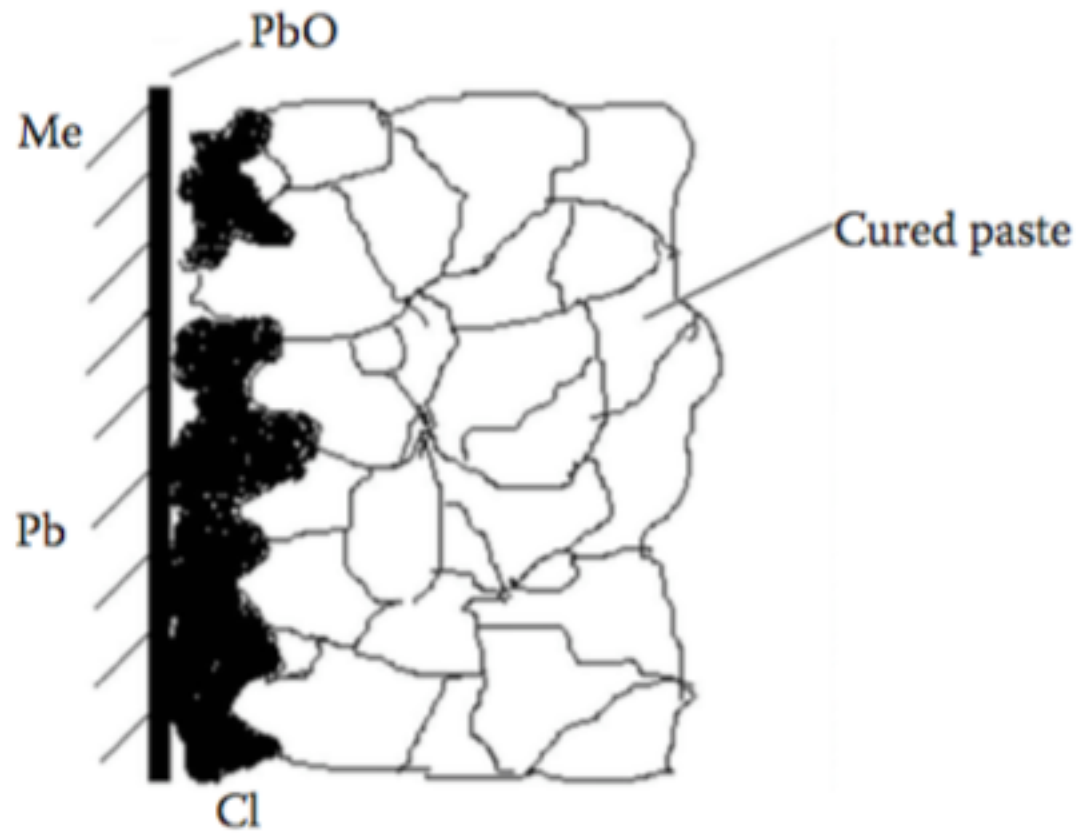


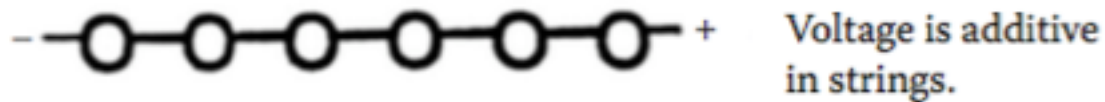
FIGURE 3.4 Scheme of the grid/PAM interface where a corrosion layer is formed during the curing process. (From M. Dimitrov, and D. Pavlov, *J. Power Sources*, 93, 234, 2001.)

4.7.2 DEEP-CYCLE BATTERIES

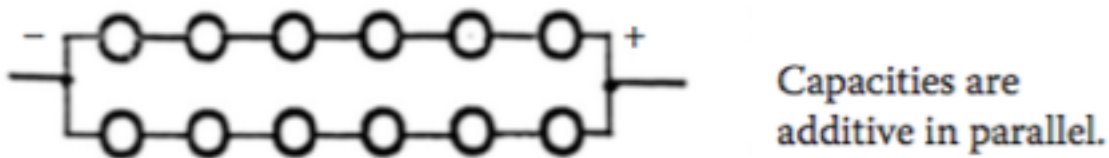
In deep-cycle batteries, two general trends have been observed. First, AGM batteries have found growth opportunities because they demonstrate low or no water loss, have the ability to prevent acid stratification, positively support the positive active material, and prevent shedding. In these same applications, a high resistance to heat, the ability to prevent soft shorts, and lower costs are normally associated with flooded battery designs and the separators utilized. Obviously, the best designed battery would combine all of the aforementioned attributes and the separator appears to be one of the primary paths to realize these goals. As with all design modifications, desired properties need to be prioritized for each individual application because trade-offs are likely between attribute performances and component costs. At the same time, other avenues will be pursued to modify the lead-acid chemistry or other electrochemical systems.

Consider a 12 V/10 Ah battery. How can we build it?

Series string: Six 2 V/10 Ah cells in series.



Parallel strings: Two 2 V/5 Ah 6-cell strings in parallel.



Parallel matrix: Five 2 V/2 Ah 6-cell strings in parallel with cross-matrixing.

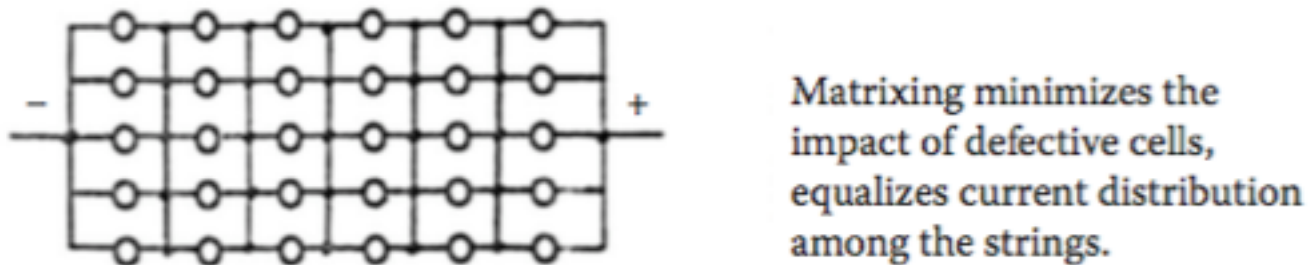


FIGURE 10.3 Battery configurations for charging. (From R. F. Nelson, *Lecture Course on VRLA*, Beijing, China, 2003.)

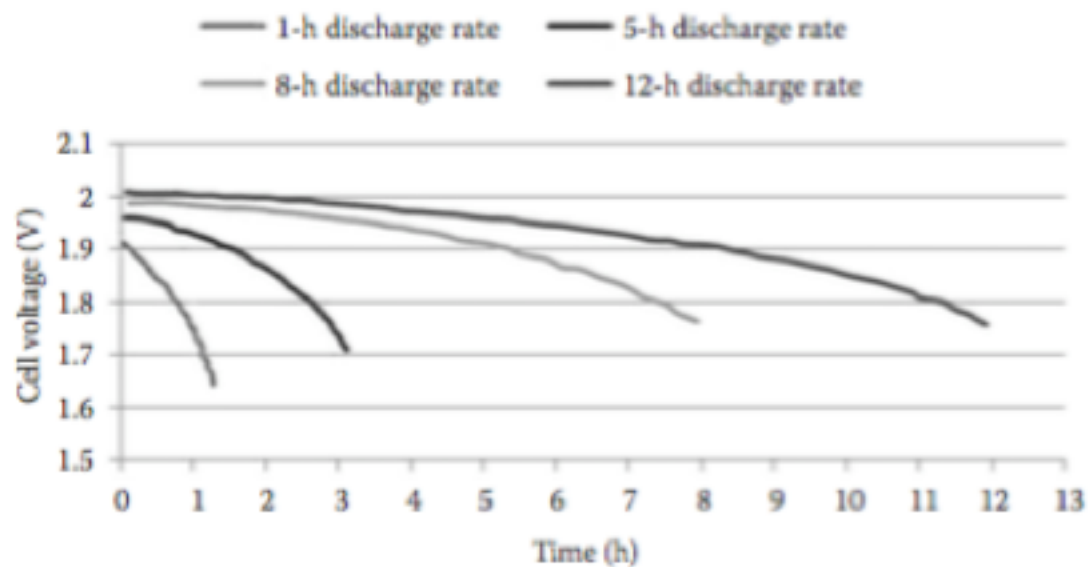


FIGURE 1.10 Discharge voltage curves for a 12-V SLI battery for different discharge currents at 25°C. (*Lead-Acid Battery, Electrochemical Technologies for Energy Storage and Conversion*, Chapter 4. 2012. Copyright Wiley-VCH Verlag GmbH & Co. KGaA. Reproduced with permission.)

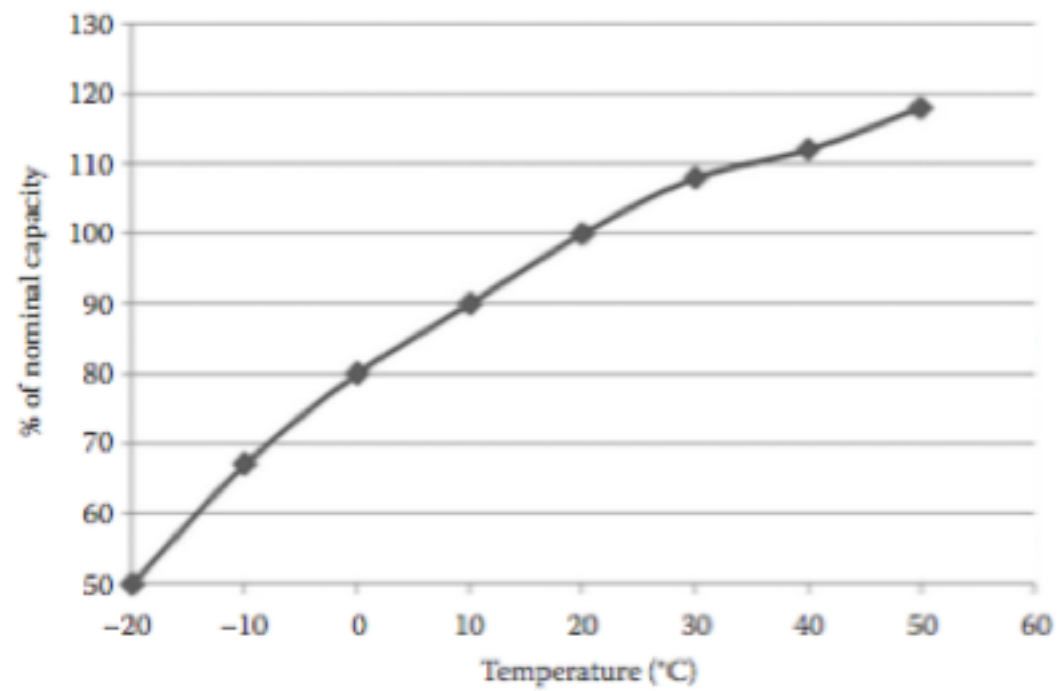
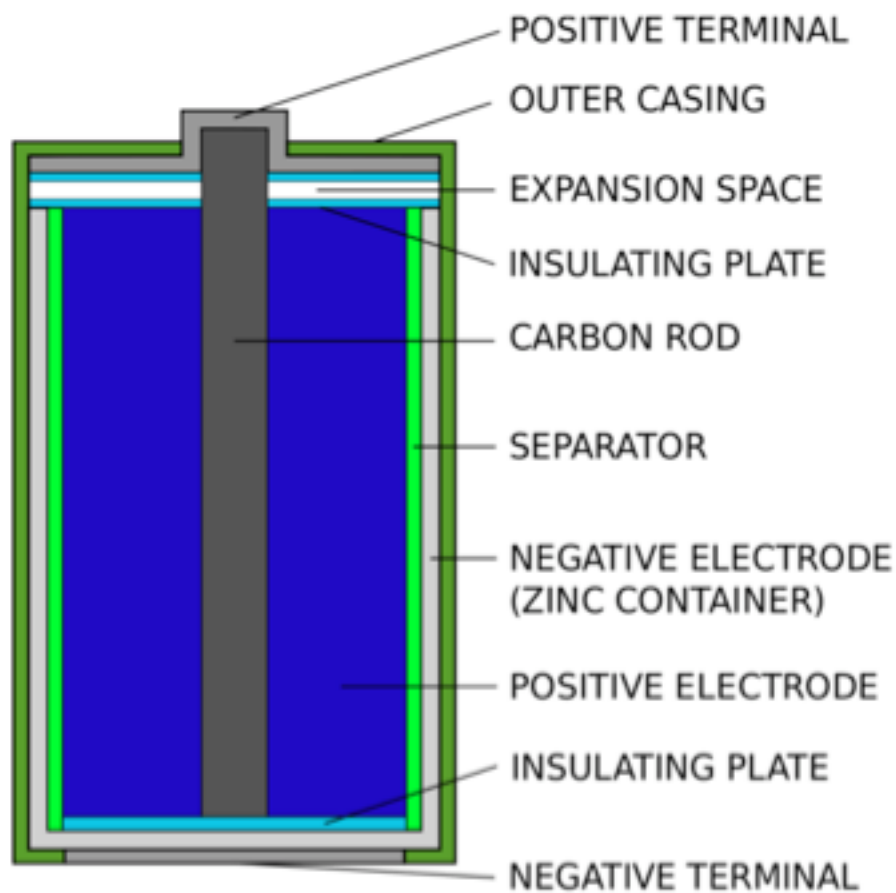


FIGURE 1.13 Capacity (10-h discharge rate) versus temperature.

Dry Cells

Many common batteries, such as those used in a flashlight or remote control, are voltaic dry cells. These batteries are called dry cells because the electrolyte is a paste. They are relatively inexpensive, but do not last a long time and are not rechargeable.



Alkaline Dry Cell

A zinc-carbon dry cell.

In the zinc-carbon dry cell, the anode is a zinc container, while the cathode is a carbon rod through the center of the cell. The paste is made of manganese(IV) oxide (MnO_2), ammonium chloride (NH_4Cl), and zinc chloride (ZnCl_2) in water. The half-reactions for this dry cell are:

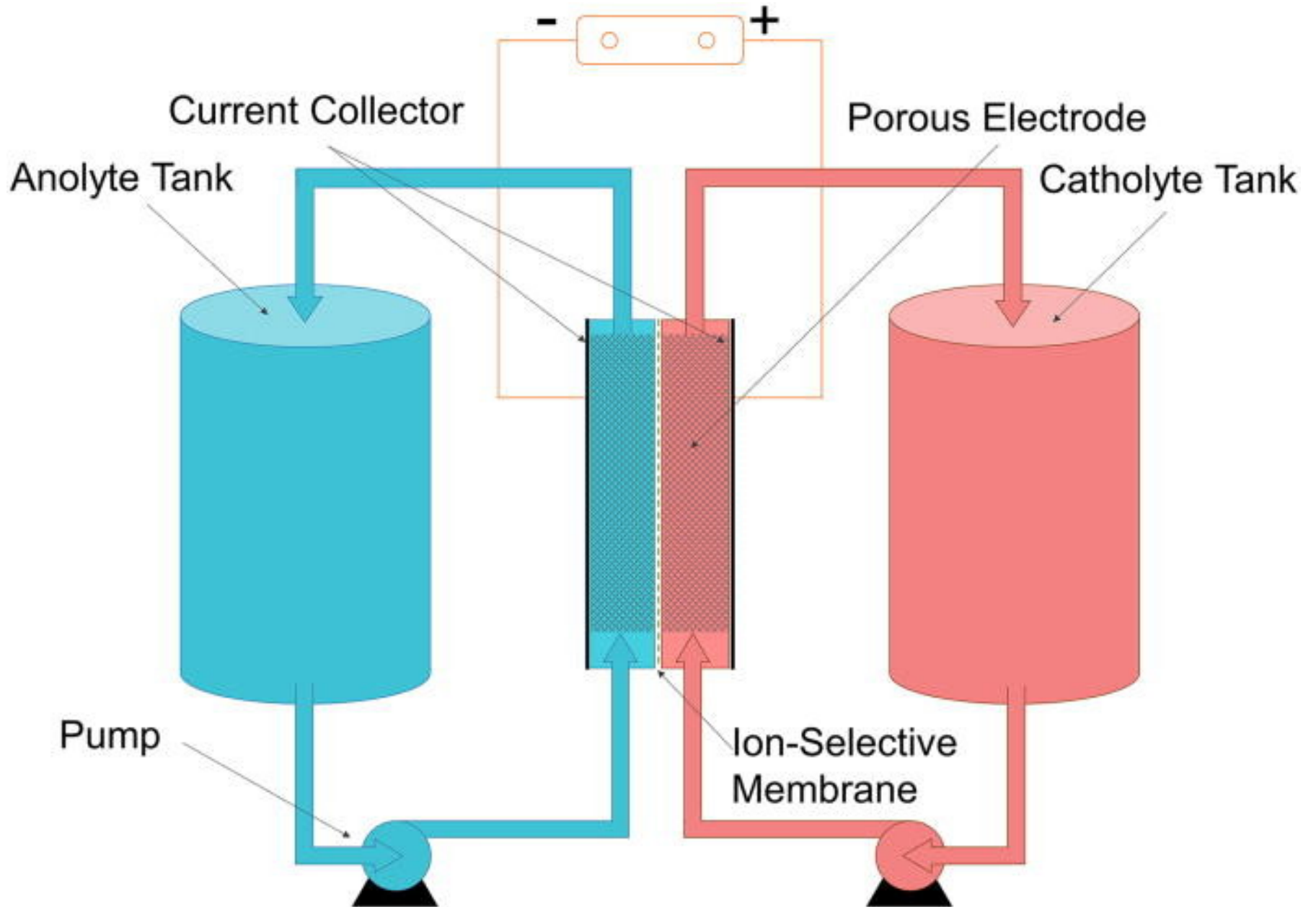


The paste prevents the contents of the dry cell from freely mixing, so a salt bridge is not needed. The carbon rod is a conductor only and does not undergo reduction. The voltage produced by a fresh dry cell is 1.5 V, but decreases during use.

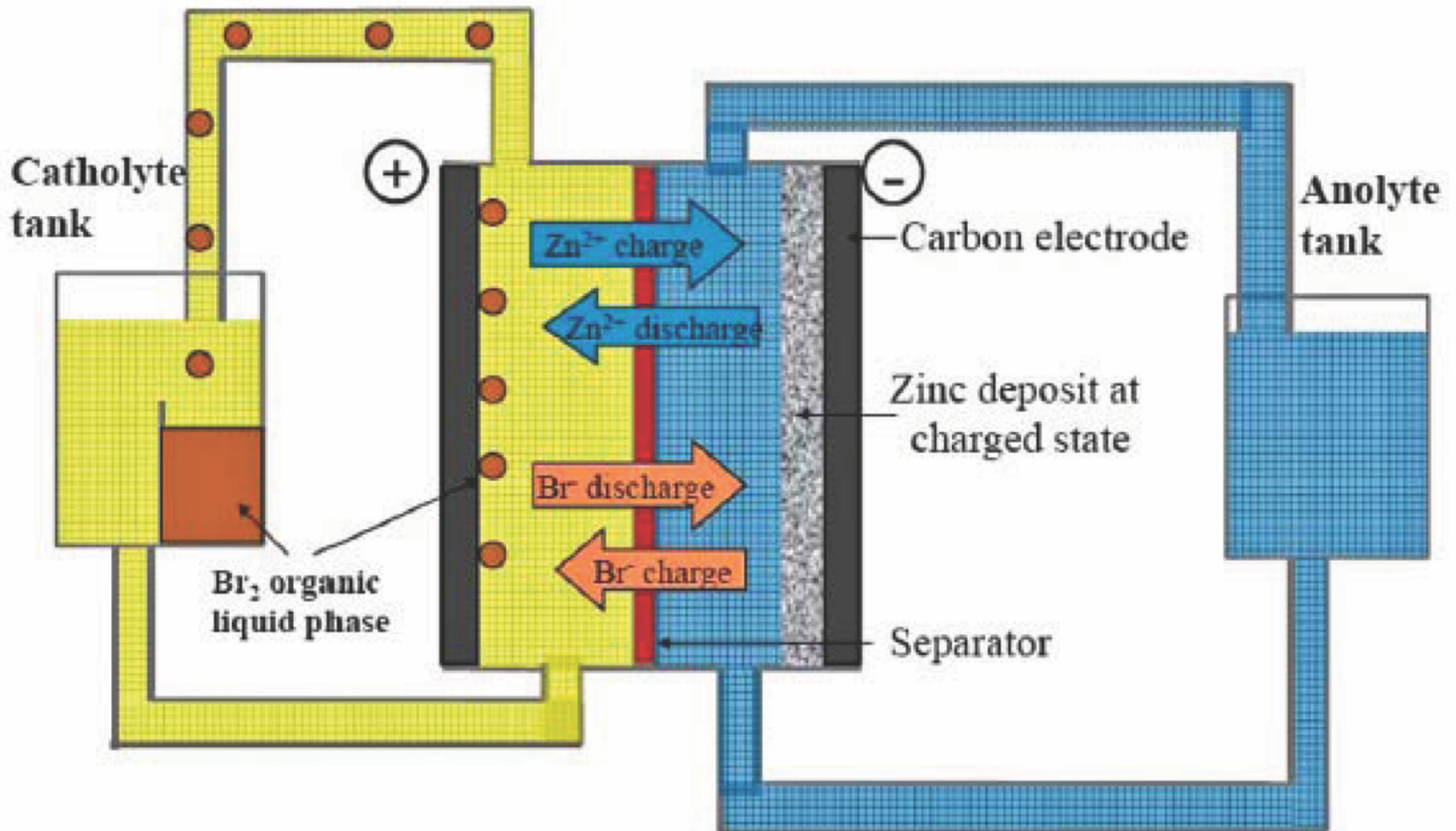
An alkaline battery is a variation on the zinc-carbon dry cell. The alkaline battery has no carbon rod and uses a paste of zinc metal and potassium hydroxide instead of a solid metal anode. The cathode half-reaction is the same, but the anode half-reaction is different.



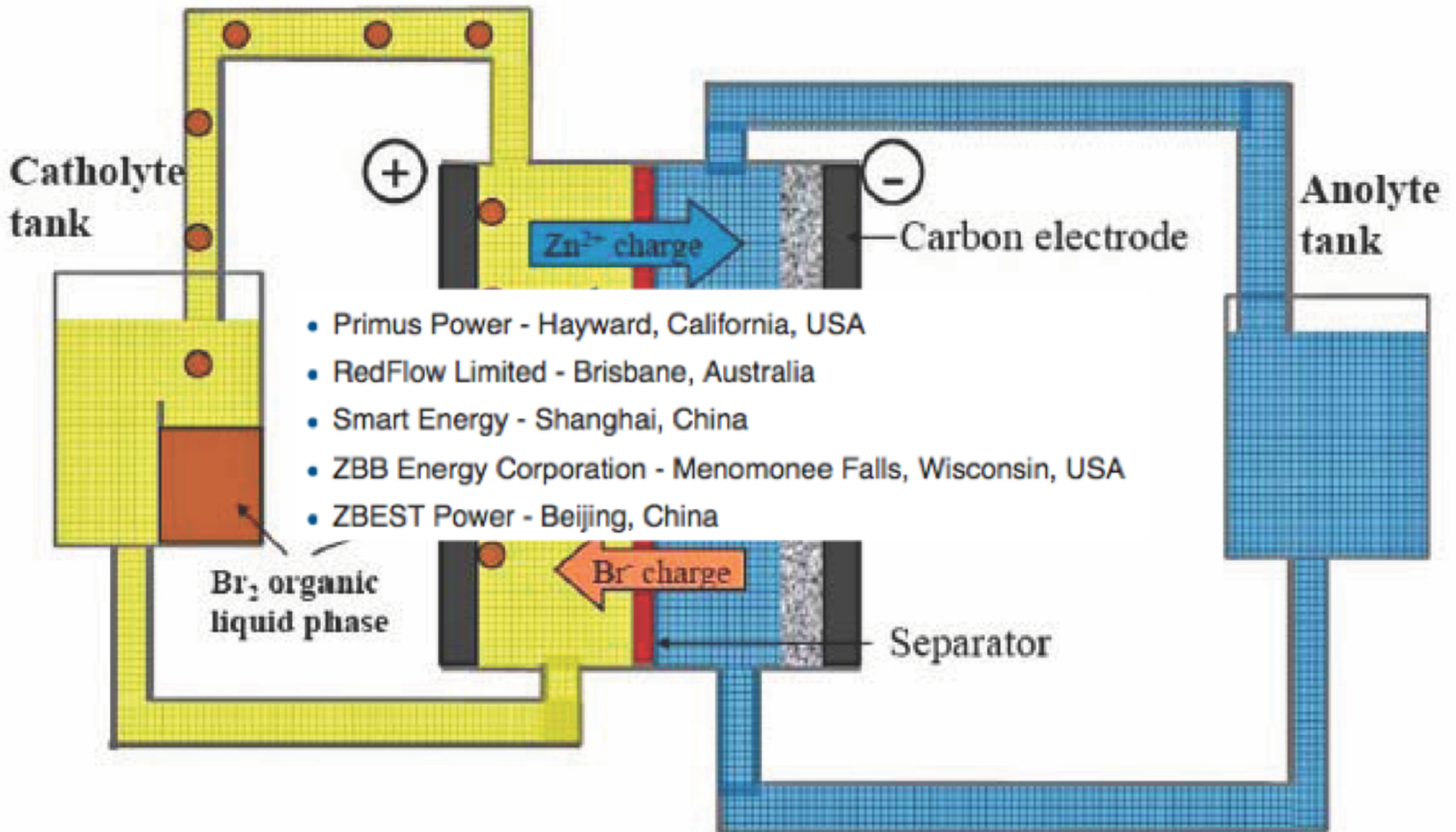
Flow Cells (Flow Batteries)



Zinc Bromide Flow Cell

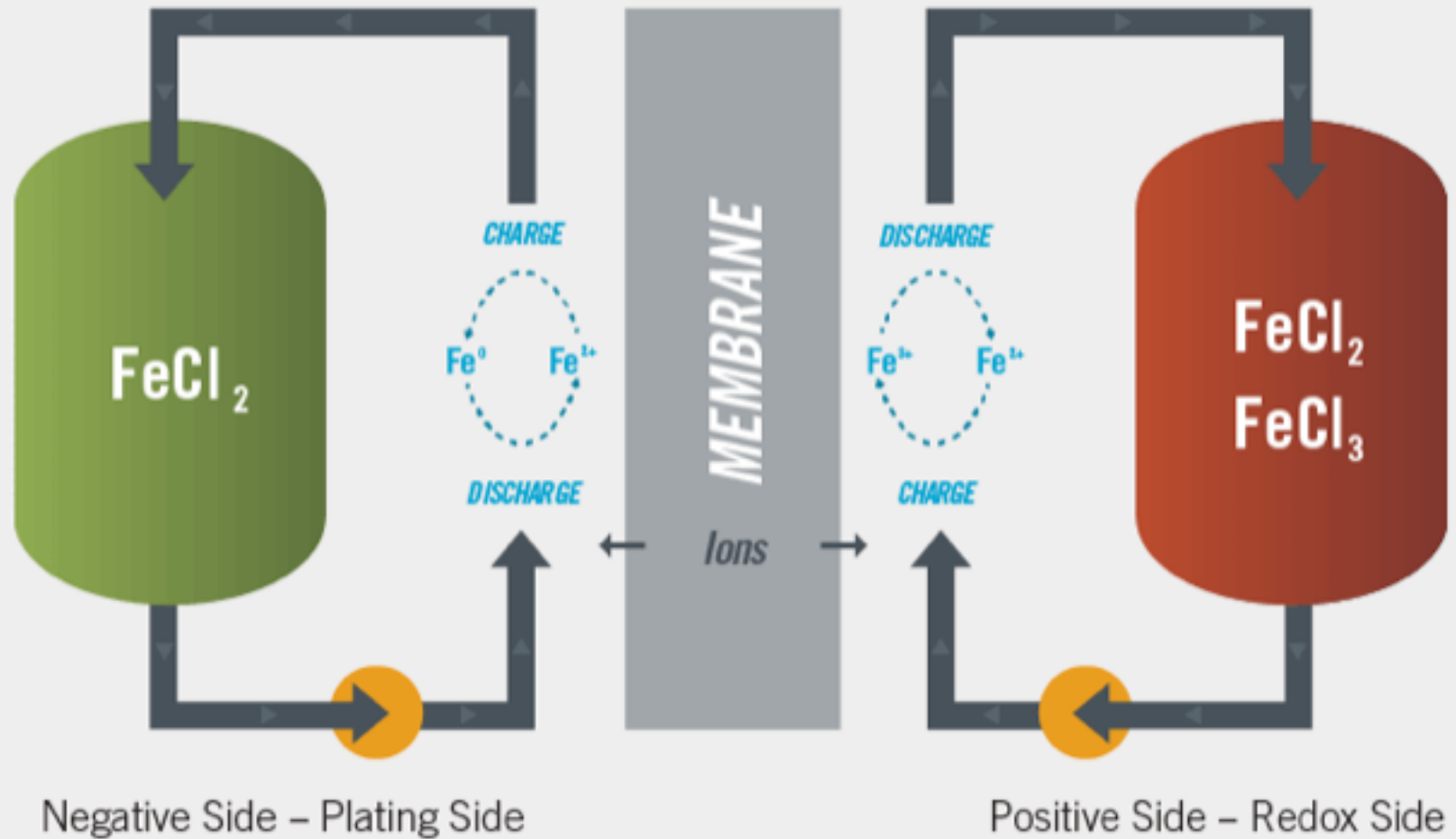


Zinc Bromide Flow Cell



Iron Water Flow Cell

How It Works: A Simple Transfer of Electrons Changed Everything



ARTICLE

Received 24 Oct 2014 | Accepted 14 Jan 2015 | Published 24 Feb 2015

DOI: 10.1038/ncomms7303

OPEN

Ambipolar zinc-polyiodide electrolyte for a high-energy density aqueous redox flow battery

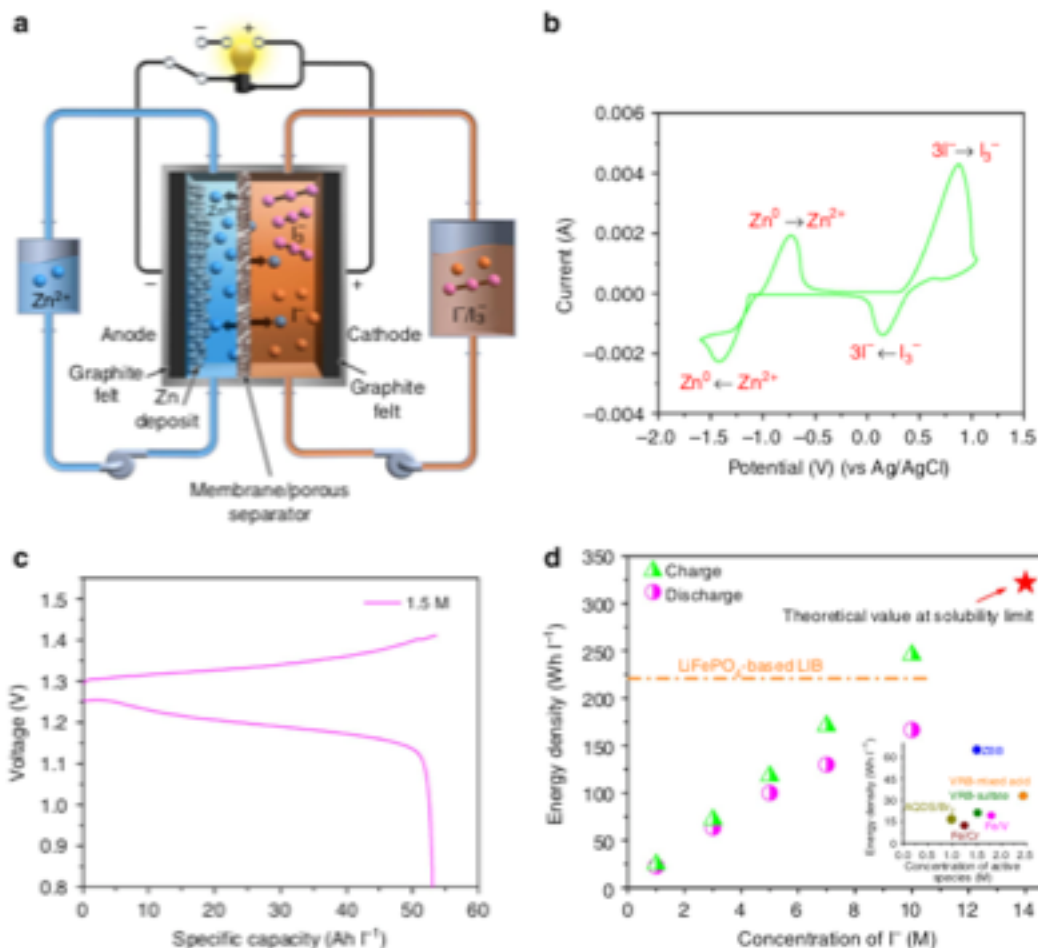
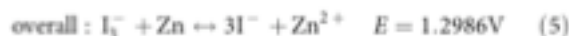
Bin Li¹, Zimin Nie¹, M. Vijayakumar², Guosheng Li¹, Jun Liu², Vincent Sprenkle³ & Wei Wang²PNL
Zinc Polyiodide
Cell

Figure 1 | Zn-I RFB and its electrochemical performance. (a) Schematic representation of the proposed ZIB system. (b) CV of 0.085M ZnI_2 on a glassy carbon electrode at the scan rate of 50 mV s^{-1} . (c) Typical charge-discharge curves at 1.5M ZnI_2 at a current density of 20 mA cm^{-2} . (d) The charge and discharge energy densities as a function of the concentration of I^- . The inset lists concentration versus energy density of several current aqueous RFB chemistries for comparison^{3,6-8}.

Table 1 | ZIB performance as a function of ZnI_2 concentration.

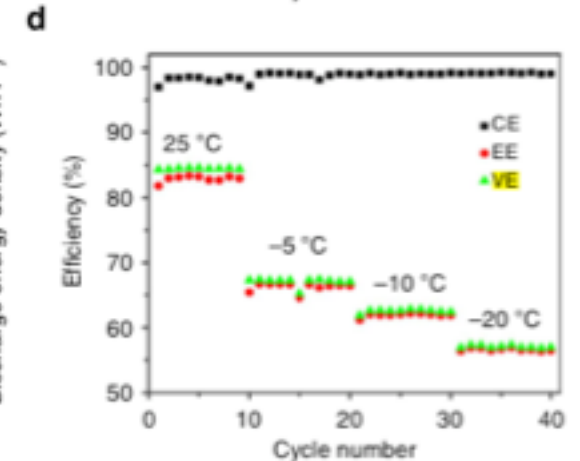
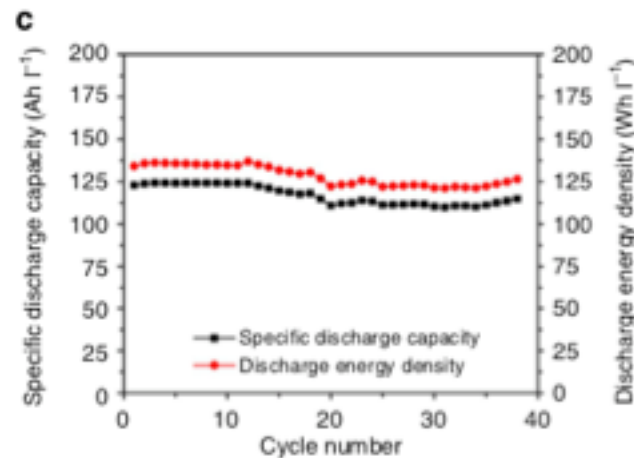
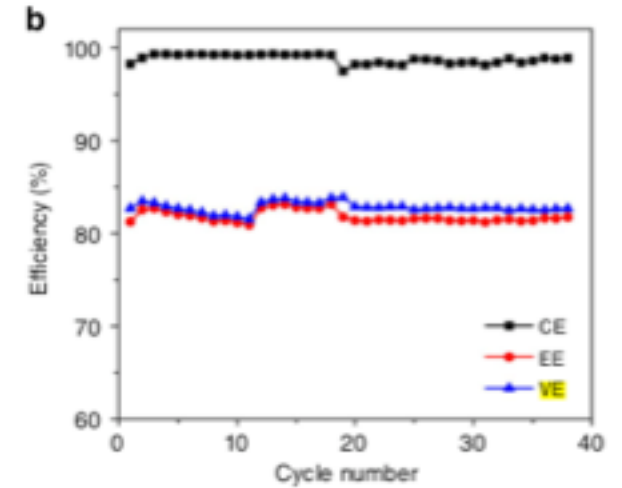
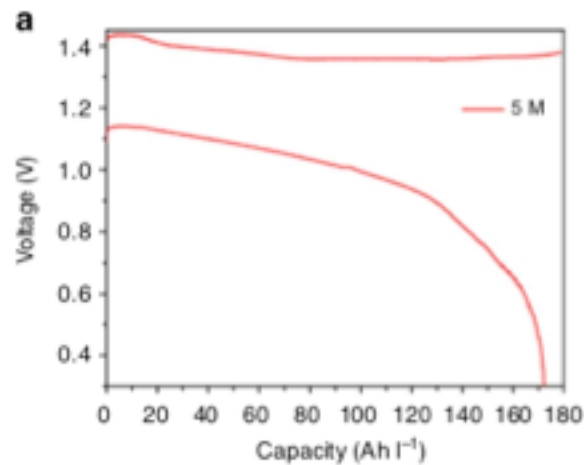
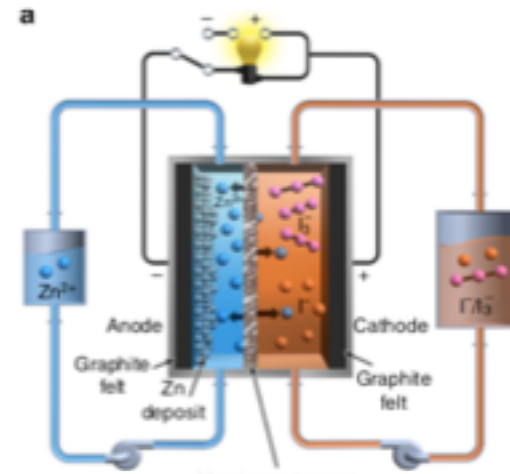
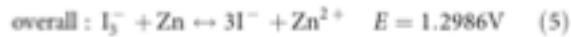
ZnI_2 (M)	CE (%)	VE (%)	EE (%)	OCV (V)	Avg. charge voltage (V)	Avg. discharge voltage (V)
0.5	99.5	91.3	90.9	1.430	1.399	1.265
1.5	99.3	88.7	88.2	1.330	1.343	1.185
2.5	99.0	85.7	84.8	1.285	1.321	1.132
3.5	99.2	76.6	76.0	1.270	1.362	1.066
5.0	96.3	70.4	67.8	1.220	1.330	0.960

CE, coulombic efficiency; EE, energy efficiency; OCV, open-circuit voltage; VE, voltage efficiency.

Ambipolar zinc-polyiodide electrolyte for a high-energy density aqueous redox flow battery

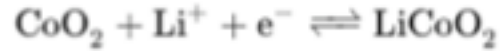
Bin Li¹, Zimin Nie¹, M. Vijayakumar², Guosheng Li¹, Jun Liu², Vincent Sprenkle³ & Wei Wang²

PNL Zinc Polyiodide Cell

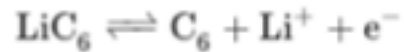


Lithium Ion Battery

The positive electrode (cathode) half-reaction in the lithium-doped cobalt oxide substrate is:^{[90][91]}



The negative electrode (anode) half-reaction for the graphite is:



The full reaction (left to right: discharging, right to left: charging) being:

